extreme strong evidence of CPV in baryon-anti-baryon pair production processes of heavy hadron decays

Zhen-Hua Zhang (张振华)
University of South China (南华大学)
based on 2504.19228, by ZZ， Jian-Yu Yang, Xin-Heng Guo

The 26th International Symposium on Spin Physics 2025.9.21-26
Shandong University, Qingdao, China

1. motivations

CPV and Matter-anti-Matter Asymmetry of the Universe

A. Sakharov's criteria

- B-violation;
- C, and CP violation;
- out of thermal equilibrium.

Santandar Model of PP:

- sphaleron transitions;
- CKM matrix for CPV mechanism (but by far not enough).

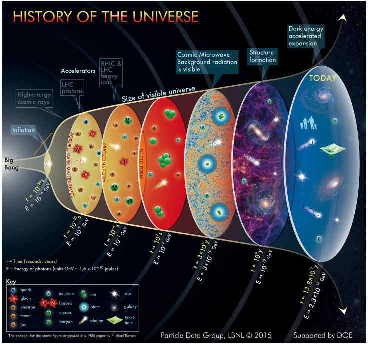

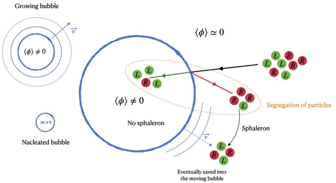

Figure 8. Sketch of electroweak baryogenesis based on nucleated bubbles and their growth. In this sketch, an equal amount of left-handed particles and right-handed antiparticles are considered (the right-handed particles and left-handed antiparticles are not participating in a sphaleron process). After particles are segregated—this is the chiral asymmetry—they are converted into a baryon asymmetry before being swallowed by the fast moving bubble.

CPV in hadron decay

story incomplete, but more interesting

- pure mesonic processes: CPV has been observed in K, B, and D meson sectors
- baryonic decays: small CPV observed in $\Lambda_b \to pK^-\pi^+\pi^-$ ($A_{CP} = (2.45 \pm 0.47)\%$), but detailed dynamics unclear. (Nature643(2025), 1223, see Yanxi's plenary talk on Friday)
- baryon-anti-baryon ($\mathcal{B}\overline{\mathcal{B}'}$) production processes: No CPV was confirmed.

Towards M. Everest.

Cronin and Fitch

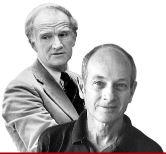

Kobayashi (小林)、Maskawa (益川)

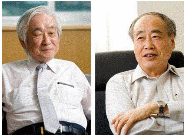

penguin diagram

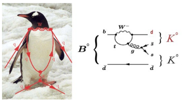

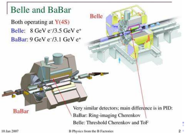

LHCb

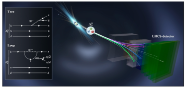

When CPV meets SPIN:

CPV in decay-angular-distributions in multi-body decays

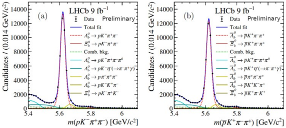

- CPV in baryon decays $\Lambda_b \to pK^-\pi^+\pi^-$: small overall CPA:

$$A_{CP} \equiv \frac{\Gamma_{\Lambda_b \to pK^-\pi^+\pi^-} - \Gamma_{\overline{\Lambda_b} \to \overline{p}K^+\pi^+\pi^-}}{\Gamma_{\Lambda_b \to pK^-\pi^+\pi^-} + \Gamma_{\overline{\Lambda_b} \to \overline{p}K^+\pi^+\pi^-}} = (2.45 \pm 0.46 \pm 0.10)\%,$$

  larger regional CPA in Dalitz regions $\Lambda_b \to R(\to p\pi^+\pi^-)K^-$:

$$A_{CP}^{\text{reg.}} = (5.4 \pm 0.9 \pm 0.1)\%.$$

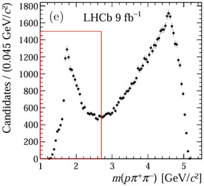

- CPV in angular correlations: no experimental evidence of Triple-Product Asymmetry induced CPAs
- a full angular-correlation analysis of CPAs is absent for four-body decays.

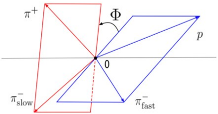

2 CPV in the angular correlations in four-body decays of heavy hadrons

Kinematics

cascade decay $H_Q \to a_k(\to 12)b_m(\to 34)$

intermediate resonances a_k's (and b_m's) with different Spin-Parities

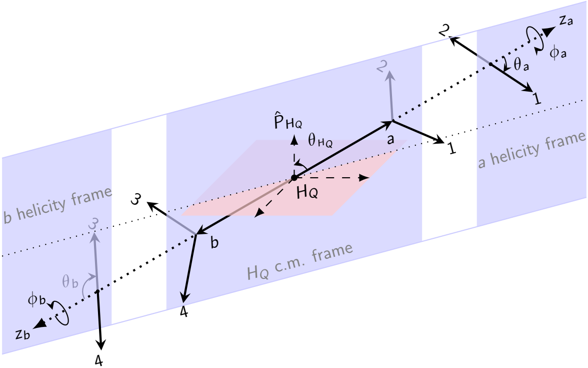

Figure: Five kinematic angles for the decay $H_Q \to a_k(\to 12)b_m(\to 34)$.

Dynamics

cascade decay $H_Q \to a_k(\to 12)b_m(\to 34)$

Decay amplitude squared for $H_Q \to a_k(\to 12)b_m(\to 34)$

$$\overline{|\mathcal{A}|^2} \propto \sum_{\sigma_a\sigma_{a'}\sigma_b\sigma_{b'}} \sum_{j_a} \sum_{j_b} \gamma^{j_a j_b}_{\sigma_a\sigma_b\sigma_{a'}\sigma_{b'}} \Omega^{j_a j_b}_{\sigma_a\sigma_b\sigma_{a'}\sigma_{b'}},$$

The kinematical factors

$$\Omega^{j_a j_b}_{\sigma_a\sigma_b\sigma_{a'}\sigma_{b'}} \equiv P_{\sigma_{ab},\sigma_{a'b'}}(\theta_{H_Q}) d^{j_a}_{\sigma_{a'a},0}(\theta_a) d^{j_b}_{\sigma_{b'b},0}(\theta_b) e^{i(\bar{\sigma}\varphi+\hat{\sigma}\phi)},$$

For unpolarized H_Q: The kinematical factors merge into (kine. angles $5 \to 3$)

$$\overline{|\mathcal{A}|^2} \propto \sum_{j_a,j_b,\sigma} \left[\Re(\gamma^{j_a j_b}_{\sigma})\Psi^{j_a j_b}_{\sigma} - \Im(\gamma^{j_a j_b}_{\sigma})\Phi^{j_a j_b}_{\sigma}\right],$$

$$\Omega^{j_a j_b}_{\sigma} = \Psi^{j_a j_b}_{\sigma} + i\Phi^{j_a j_b}_{\sigma} = d^{j_a}_{\sigma,0}(\theta_a) d^{j_b}_{\sigma,0}(\theta_b) e^{i\sigma\varphi}.$$

j_a: quantum number of $\vec{S}_{a_k} + \vec{S}_{a_{k'}}$.

$$\sigma = \sigma_a - \sigma_{a'}$$

Angular correlations

Table: The first few angular correlations.

j_a \ j_b	0	1	2
0	$\Psi_0^{00} = 1$ trivial	$\Psi_0^{01} c_{\theta_b}$	$\Psi_0^{02} = \frac{1}{2}(c_{\theta_b}^2 - 1)$
1	$\Psi_0^{10} = c_{\theta_a}$	$\Psi_0^{11} = c_{\theta_a} c_{\theta_b}$ $\Psi_1^{11} = s_{\theta_a} s_{\theta_b} c_{\varphi}$ $\Phi_1^{11} = s_{\theta_a} s_{\theta_b} s_{\varphi}$	$\Psi_0^{12} = \frac{1}{2} c_{\theta_a}(3c_{\theta_b}^2 - 1)$ $\Psi_1^{12} = s_{\theta_a} s_{\theta_b} c_{\theta_b} c_{\varphi}$ $\Phi_1^{12} = s_{\theta_a} s_{\theta_b} c_{\theta_b} s_{\varphi}$
2	$\Psi_0^{20} = \frac{1}{2}(3c_{\theta_a}^2 - 1)$	$\Psi_0^{21} = \frac{1}{2}(3c_{\theta_a}^2 - 1) c_{\theta_b}$ $\Psi_1^{21} = s_{\theta_a} c_{\theta_a} s_{\theta_b} c_{\varphi}$ $\Phi_1^{21} = s_{\theta_a} c_{\theta_a} s_{\theta_b} s_{\varphi}$	$\Psi_0^{22} = \frac{1}{4}(3c_{\theta_a}^2 - 1)(3c_{\theta_b}^2 - 1)$ $\Psi_1^{22} = s_{\theta_a} c_{\theta_a} s_{\theta_b} c_{\theta_b} c_{\varphi}$ $\Phi_1^{22} = s_{\theta_a} c_{\theta_a} s_{\theta_b} c_{\theta_b} s_{\varphi}$ $\Psi_2^{22} = \frac{3}{8} s_{\theta_a}^2 s_{\theta_b}^2 c_{2\varphi}$ $\Phi_2^{22} = \frac{3}{8} s_{\theta_a}^2 s_{\theta_b}^2 s_{2\varphi}$

Kinematics $\leftrightarrow$ Dynamics

cascade decay $H_Q \to a_k(\to 12)b_m(\to 34)$

Constraints to j_a and j_b

- Triangular inequality

$$|s_{a_k} - s_{a_{k'}}| \leqslant j_a \leqslant s_{a_k} + s_{a_{k'}}.$$

- Parity symmetry in the strong decay $a \to 12$

$$(-)^{j_a} = \Pi_{a_k}\Pi_{a_{k'}},$$

If let a_k and $a_{k'}$ run over all the allowed possibilities, we obtain all the allowed values of j_a.

Inversely, if possible j_a (and j_b) is seen from the data, we can infer what kind of resonances enters.

Kinematics $\leftrightarrow$ Dynamics (interference pattern)

Kinematics $\leftrightarrow$ Dynamics

CPA inducde by Interference between intermediate resonances

Resonance-Interference

- I. CPAs in angular distributions
- II. complementary CPA observables

Kinematics ↔ Dynamics

Resonance-Interference: I. CPAs in angular distributions (cancellation type I)

Forward-Backward Asymmetry induced CPA (FB-CPA)

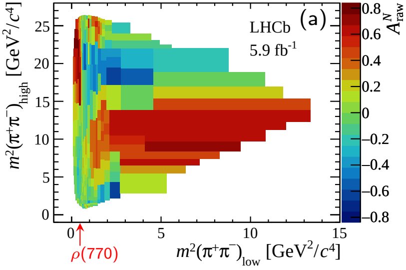

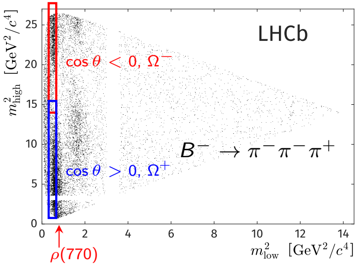

$$A^{FB}_{B^-} = \frac{N^{\Omega^+}_{B^-} - N^{\Omega^-}_{B^-}}{N^{\Omega^+}_{B^-} + N^{\Omega^-}_{B^-}} = \frac{\Re(\langle a_S^* a_P e^{i\delta}\rangle)}{|\langle a_P\rangle|^2/3 + |\langle a_S\rangle|^2}.$$

$$A^{FB}_{CP} = \frac{1}{2}(A^{FB}_{B^-} - A^{FB}_{B^+})$$

ZZ, X.-H. Guo, and Y.-D. Yang, [PRD87, 076007 (2013)]

ZZ, PLB820, 136537

Y.-R. Wei, ZZ, PRD 106(2022), 113002

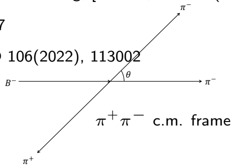

Kinematics $\leftrightarrow$ Dynamics

Resonance-Interference: I. CPAs in angular distributions

CPV in baryon-four-body decays: $\Lambda_b^0 \to p\pi^-\pi^+\pi^-$ $N(1440) - N(1520)$ and $f_0(500) - \rho(770)$, ZZ, PRD107(2023),L011301

$\Lambda_b^0 \to N(\to p\pi^-)f/\rho(\to \pi^+\pi^-)$: c_{θ_a} and c_{θ_b} are correlated.

$$(\Gamma_{jl}) \sim \left(\begin{array}{c|c|c} \text{Non-int} & (N_{1440}N_{1520})|f|^2,\ (N_{1440}N_{1520})|\rho|^2 & \text{Non-int} \\ \hline (f\rho)|N_{1440}|^2,\ (f\rho)|N_{1520}|^2 & (N_{1440}N_{1520}f\rho)_{GI} & (f\rho)|N_{1520}|^2 \\ \hline \text{Non-int} & (N_{1440}N_{1520})|\rho|^2 & \text{Non-int} \end{array}\right).$$

GI term corresponding to $\cos\theta_a \cos\theta_b$

2 Dim Phase Space

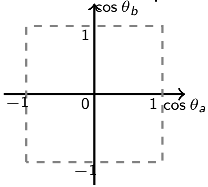

two-fold FBA (TFFBA): $j = 1 = l$

$$\tilde{A}^{11} = \frac{(N_I - N_{II} + N_{III} - N_{IV})}{N}$$

TFFBA-CPA

$$A_{CP}^{11} = \frac{1}{2}(\tilde{A}^{11} - \overline{\tilde{A}^{11}})$$

Kinematics ↔ Dynamics

Resonance-Interference: I. CPAs in angular distributions

Partial-Wave CPAs

$$\overline{|\mathcal{M}|^2} = \sum_j P_j(c_{\theta_1'}) w^{(j)}.$$

$$w^{(j)} = \sum_{ii'} \left\langle \frac{\mathcal{S}_{ii'}^{(j)} \mathcal{W}_{ii'}^{(j)}}{\mathcal{I}_{R_i} \mathcal{I}_{R_{i'}}} \right\rangle,$$

$$\mathcal{W}_{ii'}^{(j)} = \sum_{\sigma \lambda_3} (-)^{\sigma - s} \langle s_{R_i} - \sigma s_{R_{i'}} \sigma | s_{R_i} s_{R_{i'}} j0 \rangle \mathcal{F}^J_{R_i, \sigma \lambda_3} \mathcal{F}^{J*}_{R_{i'}, \sigma \lambda_3},$$

$$\mathcal{S}_{ii'}^{(j)} = \sum_{\lambda_1' \lambda_2'} (-)^{s - \lambda'} \langle s_{R_i} - \lambda' s_{R_{i'}} \lambda' | s_{R_i} s_{R_{i'}} j0 \rangle \mathcal{F}^{R_i, s_{R_i}}_{\lambda_1' \lambda_2'} \mathcal{F}^{R_{i'}, s_{R_{i'}} *}_{\lambda_1' \lambda_2'}$$

$$A^j_{CP} = \frac{w^j - \overline{w}^j}{w^j + \overline{w}^j}$$

ZHZ, X.-H. Guo, JHEP07(2021)177

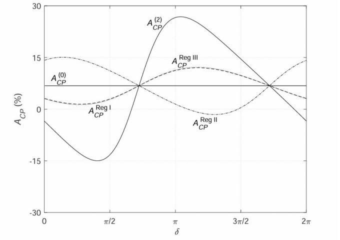

Figure 1. The PW*CP*A $A_{CP}^{(2)}$ (solid curvy line) for $\Lambda_b^0 \to p\pi^-\pi^+\pi^-$ near the resonance $\Delta^0(1232)$ as a function of the strong phase δ. The regional *CP* asymmetry $A_{CP}^{(0)}$ (solid straight line), $A_{CP}^{\text{Reg I}}$ (dotted line), $A_{CP}^{\text{Reg II}}$ (dash-dotted line), and $A_{CP}^{\text{Reg III}}$ (dashed line) are also shown for comparison. The difference between $A_{CP}^{\text{Reg I}}$ and $A_{CP}^{\text{Reg III}}$ is very tiny. Other PW*CP*As $A_{CP}^{(1)}$ and $A_{CP}^{(3)}$ are not shown due to the reason explained in the text. The invariant mass squared $s_{p\pi}$ is integrated from $(m_\Delta - \Gamma_\Delta)^2$ to $(m_\Delta + \Gamma_\Delta)^2$.

Kinematics ↔ Dynamics

Resonance-Interference: II. complementary CPA observables

The interfering term

$$\Re\left(\frac{\mathcal{A}_r\mathcal{B}^*}{s_r}\right) = \frac{\Re\left(\mathcal{A}_r\mathcal{B}^*\right)\left(s - m_r^2\right) + \Im\left(\mathcal{A}_r\mathcal{B}^*\right) m_r\Gamma_r}{\left|s_r\right|^2}.$$

a pair of complementary CPV observables

$$A_{CP} \equiv \frac{\int_{{m_r}^2-\Delta_-}^{{m_r}^2+\Delta_+}\left(\overline{|\mathcal{M}|^2} - \overline{\left|\overline{\mathcal{M}}\right|^2}\right) ds}{\int_{{m_r}^2-\Delta_-}^{{m_r}^2+\Delta_+}\left(\overline{|\mathcal{M}|^2} + \overline{\left|\overline{\mathcal{M}}\right|^2}\right) ds} \sim \sin\delta\sin\phi \quad \text{mainly from } \Im\left(\mathcal{A}_r\mathcal{B}^*\right)$$

$$\tilde{A}_{CP} \equiv \frac{\int_{{m_r}^2-\Delta_-}^{{m_r}^2+\Delta_+}\left(\overline{|\mathcal{M}|^2} - \overline{\left|\overline{\mathcal{M}}\right|^2}\right) \operatorname{sgn}\left(s - {m_2'}^2\right) ds}{\int_{{m_r}^2-\Delta_-}^{{m_r}^2+\Delta_+}\left(\overline{|\mathcal{M}|^2} + \overline{\left|\overline{\mathcal{M}}\right|^2}\right) ds} \sim \cos\delta\sin\phi \quad \text{mainly } \Re\left(\mathcal{A}_r\mathcal{B}^*\right)$$

$$A_{CP}^2 + \tilde{A}_{CP}^2 \sim \#\sin^2\phi$$

Kinematics $\leftrightarrow$ Dynamics

Resonance-Interference: II. complementary CPA observables

LHCb, PRD 101 (2020) 012006 [1909.05212]

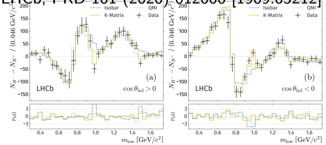

Figure 12: Raw difference in the number of B^- and B^+ candidates in the low $m_{\rm low}$ region, for (a) positive, and (b) negative cosine of the helicity angle. The pull distribution is shown below each fit projection.

$$A^{FB}_{CP,k} = \frac{(N_{B^-} - N_{B^+})_{\cos\theta_{\rm hel}>0,k} - (N_{B^-} - N_{B^+})_{\cos\theta_{\rm hel}<0,k}}{(N_{B^-} + N_{B^+})_{\cos\theta_{\rm hel}>0,k} + (N_{B^-} + N_{B^+})_{\cos\theta_{\rm hel}<0,k}}$$

$$A^{FB,{\rm ave}}_{CP} = \frac{\sum_{k=8}^{15}[(N_{B^-} - N_{B^+})_{\cos\theta_{\rm hel}>0,k} - (N_{B^-} - N_{B^+})_{\cos\theta_{\rm hel}<0,k}]}{\sum_{k=8}^{15}[(N_{B^-} + N_{B^+})_{\cos\theta_{\rm hel}>0,k} + (N_{B^-} + N_{B^+})_{\cos\theta_{\rm hel}<0,k}]} = (0.8 \pm 1.0)\%$$

J.-J. Qi, J.-Y. Yang, ZZ, PRD110(2024) L111301[2407.20586]

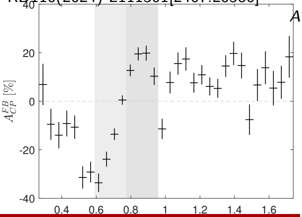

$$A^{FB,\Im}_{CP} = \frac{\left(\sum_{k=12}^{15} - \sum_{k=8}^{11}\right)\left[(N_{B^-} - N_{B^+})_{\cos\theta_{\rm hel}>0,k} - (N_{B^-} - N_{B^+})_{\cos\theta_{\rm hel}<0,k}\right]}{\sum_{k=8}^{15}\left[(N_{B^-} + N_{B^+})_{\cos\theta_{\rm hel}>0,k} + (N_{B^-} + N_{B^+})_{\cos\theta_{\rm hel}<0,k}\right]} = (13.2 \pm 1.0)\%$$

significane: $1\sigma \rightarrow 13\sigma$!

Kinematics $\leftrightarrow$ CPV observables

Angular correlation CPV observables in four-body cascade decays

Decay angular correlation CPV observables

$$A_{CP}^{\mathcal{Y}_\sigma^{j_a j_b}} \equiv \frac{\left(N_{\mathcal{Y}_\sigma^{j_a j_b}>0} - N_{\mathcal{Y}_\sigma^{j_a j_b}<0}\right) - \left(N_{\overline{\mathcal{Y}}_\sigma^{j_a j_b}>0} - N_{\overline{\mathcal{Y}}_\sigma^{j_a j_b}<0}\right)}{N + \overline{N}}.$$

Complementary CPV observables

$$\tilde{A}_{CP}^{\mathcal{Y}_\sigma^{j_a j_b}} \equiv \frac{\left[\left(N_{\mathrm{sgn}_{34}\mathcal{Y}_\sigma^{j_a j_b}>0} - N_{\mathrm{sgn}_{34}\mathcal{Y}_\sigma^{j_a j_b}<0}\right) - \left(N_{\mathrm{sgn}_{34}\overline{\mathcal{Y}}_\sigma^{j_a j_b}>0} - N_{\mathrm{sgn}_{34}\overline{\mathcal{Y}}_\sigma^{j_a j_b}<0}\right)\right]}{N + \overline{N}}.$$

CPV observables $\leftrightarrow$ Kinematics $\leftrightarrow$ Dynamics (interference pattern)

3 Discussion on LHCb results of the decay $B^0 \to p\bar{p}K^+\pi^-$

A type of decay involving baryon $B^0 \to p\bar{p}K^+\pi^-$

arXiv > hep-ex > arXiv:2205.08973

Search... Hel

High Energy Physics - Experiment

[Submitted on 18 May 2022 (v1), last revised 16 Aug 2023 (this version, v2)]

Search for CP violation using $\hat{T}$-odd correlations in $B^0 \to p\bar{p}K^+\pi^-$ decays

LHCb collaboration

A search for CP and P violation in charmless four-body $B^0 \to p\bar{p}K^+\pi^-$ decays is performed using triple-product asymmetry observables. It is based on proton-proton collision data collected by the LHCb experiment at centre-of-mass energies of 7, 8 and 13 TeV, corresponding to a total integrated luminosity of 8.4 fb^{-1}. The CP- and P-violating asymmetries are measured both in the integrated phase space and in specific regions. No evidence is seen for CP violation. P-parity violation is observed at a significance of 5.8 standard deviations

Comments:	All figures and tables, along with any supplementary material and additional information, are available at this https URL (LHCb public pages)
Subjects:	**High Energy Physics - Experiment (hep-ex)**
Report number:	LHCb-PAPER-2022-003, CERN-EP-2022-083
Cite as:	arXiv:2205.08973 **[hep-ex]**
	(or arXiv:2205.08973v2 **[hep-ex]** for this version)
	https://doi.org/10.48550/arXiv.2205.08973
Journal reference:	Phys. Rev. D108 (2023) 032007
Related DOI:	https://doi.org/10.1103/PhysRevD.108.032007

Submission history

From: Matteo Bartolini [view email]
[v1] Wed, 18 May 2022 14:54:32 UTC (517 KB)
[v2] Wed, 16 Aug 2023 12:23:37 UTC (739 KB)

"No evidence of CPV (corresponding to T-odd correlation) in $B^0 \to p\bar{p}K^+\pi^-$."

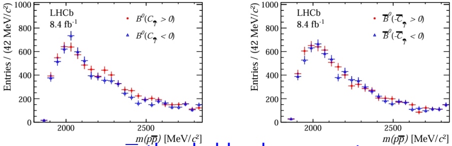

$p\bar{p}$ threshold enhancement

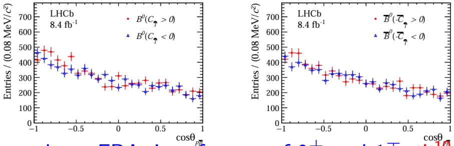

large FBA, interference of $0^{\pm}$ and $1^{\mp}$, Ψ_0^{10}

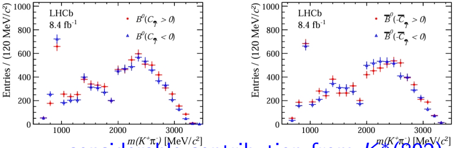

considerable contribution from $K^*(892)$

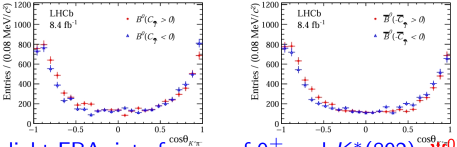

slight FBA, interference of $0^{\pm}$ and $K^*(892)$, Ψ_0^{01}

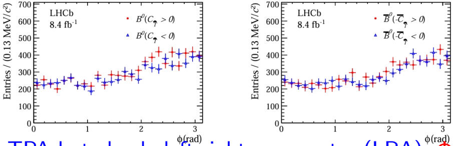

no TPA but clearly left-right asymmetry (LRA), Φ_1^{11}

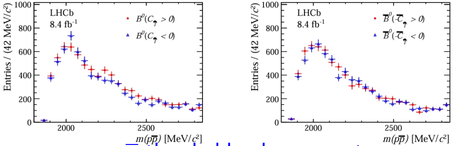

$p\bar{p}$ threshold enhancement

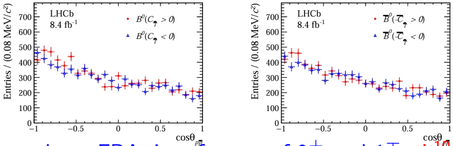

large FBA, interference of $0^\pm$ and $1^\mp$, Ψ_0^{10}

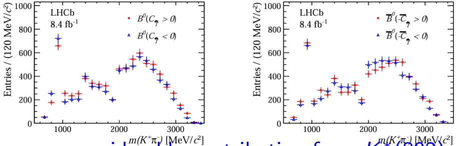

considerable contribution from $K^*(892)$

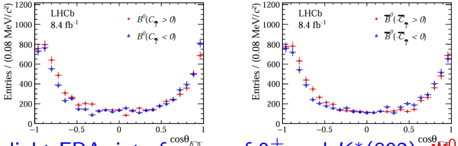

slight FBA, interference of $0^\pm$ and $K^*(892)$, Ψ_0^{01}

Ψ_0^{01}, Ψ_0^{10}, Φ_1^{11}, $\Rightarrow$ $j_a, j_b = 0, 1,$

$\Rightarrow$ $0^\pm$ & $1^\mp$, $K^*(892)$&0^+

$\Rightarrow$ $j_a, j_b = 0, 1, 2.$

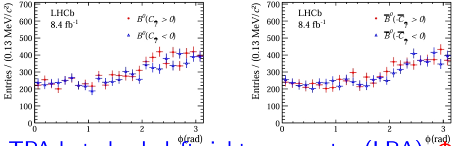

no TPA but clearly left-right asymmetry (LRA), Φ_1^{11}

angular correlations

focusing on phase space around $K^*(892)$ and the threshold region of $p\bar{p}$

j_a \ j_b	0	1	2
0	$\Psi_0^{00} = 1$ trivial	$\Psi_0^{01} c_{\theta_b}$	$\Psi_0^{02} = \frac{1}{2}(c_{\theta_b}^2 - 1)$
1	$\Psi_0^{10} = c_{\theta_a}$	$\Psi_0^{11} = c_{\theta_a} c_{\theta_b}$ $\Psi_1^{11} = s_{\theta_a} s_{\theta_b} c_\varphi$ $\Phi_1^{11} = s_{\theta_a} s_{\theta_b} s_\varphi$	$\Psi_0^{12} = \frac{1}{2} c_{\theta_a}(3c_{\theta_b}^2 - 1)$ $\Psi_1^{12} = s_{\theta_a} s_{\theta_b} c_{\theta_b} c_\varphi$ $\Phi_1^{12} = s_{\theta_a} s_{\theta_b} c_{\theta_b} s_\varphi$
2	$\Psi_0^{20} = \frac{1}{2}(3c_{\theta_a}^2 - 1)$	$\Psi_0^{21} = \frac{1}{2}(3c_{\theta_a}^2 - 1)c_{\theta_b}$ $\Psi_1^{21} = s_{\theta_a} c_{\theta_a} s_{\theta_b} c_\varphi$ $\Phi_1^{21} = s_{\theta_a} c_{\theta_a} s_{\theta_b} s_\varphi$	$\Psi_0^{22} = \frac{1}{4}(3c_{\theta_a}^2 - 1)(3c_{\theta_b}^2 - 1)$ $\Psi_1^{22} = s_{\theta_a} c_{\theta_a} s_{\theta_b} c_{\theta_b} c_\varphi$ $\Phi_1^{22} = s_{\theta_a} c_{\theta_a} s_{\theta_b} c_{\theta_b} s_\varphi$ $\Psi_2^{22} = \frac{3}{8} s_{\theta_a}^2 s_{\theta_b}^2 c_{2\varphi}$ $\Phi_2^{22} = \frac{3}{8} s_{\theta_a}^2 s_{\theta_b}^2 s_{2\varphi}$

Extracting the event yields from LHCb's paper

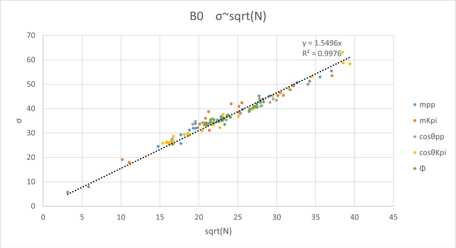

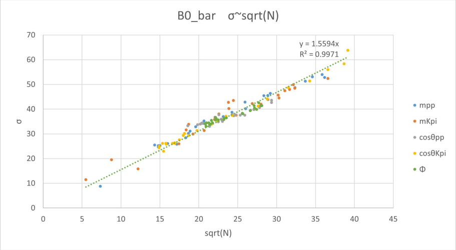

Fitting the yields and the errors from all the subfigures for B^0 and $\overline{B^0}$. The data sets in different rows of the subfigures in Fig. 5 of the LHCb's PRD paper, which are denoted with dots of different colors in our fitting figure, are in fact the same data sets but projected onto different kinematical variables. The fitting procedures should also be done separately on each projected data set. Actually, we did the separate fitting on each data set and obtained quite the same k consistently. Hence we concisely present the combined fitting in one figure.
The yields and their corresponding errors are all well aligned according to

$$N = \left(\frac{\sigma}{k}\right)^2, \quad k \approx 1.55.$$

Extracting the event yields from LHCb's paper

B^0		Scheme A			Scheme B					
					$m^2_{K\pi} - m^2_{K*} < 0$			$m^2_{K\pi} - m^2_{K*} > 0$		
sign $c_{\theta_a} c_{\theta_b} c_\varphi$	sign s_φ	bin	$A_{\hat{T}}$	yie.	bin	$A_{\hat{T}}$	yie.	bin	$A_{\hat{T}}$	yie.
$- - +$	$+$	0	-16.5 ± 10.1	98	0	-26.7 ± 17.8	28	8	-5.1 ± 12.8	70
	$-$			137			48			77
$- - -$	$+$	1	6.1 ± 9.2	150	1	5.4 ± 15.8	51	9	6.6 ± 11.6	95
	$-$			133			45			83
$- + +$	$+$	2	-1.2 ± 7.0	242	2	-7.3 ± 11.1	90	10	0.7 ± 9.0	149
	$-$			248			105			147
$- + -$	$+$	3	25.3 ± 7.2	290	3	15.4 ± 12.8	85	11	30.9 ± 8.7	208
	$-$			173			62			110
$+ - +$	$+$	4	7.8 ± 11.1	105	4	-21.9 ± 13.9	49	12	38.4 ± 16.8	59
	$-$			90			76			26
$+ - -$	$+$	5	2.9 ± 8.3	179	5	-13.4 ± 13.9	54	13	11.6 ± 10.2	129
	$-$			169			70			102
$+ + +$	$+$	6	-22.8 ± 7.4	169	6	-19.3 ± 10.4	90	14	-24.1 ± 10.5	83
	$-$			269			132			135
$+ + -$	$+$	7	-10.4 ± 6.8	233	7	0.7 ± 10.9	102	15	-18.8 ± 8.6	132
	$-$			287			100			193

Table: The TPAs in different regions from the data of LHCb, and the corresponding event yields extracted from the TPAs data for $B^0 \to p\bar{p}K^+\pi^-$. In the table, c_{θ_a}, c_{θ_b}, c_φ and s_φ are abbreviations for $\cos\theta_a$, $\cos\theta_b$, $\cos\varphi$, and $\sin\varphi$, respectively.

Extracting the event yields from LHCb's paper

$\overline{B^0}$		Scheme A			Scheme B					
sign $c_{\bar{\theta}_a}c_{\bar{\theta}_b}c_{\bar{\varphi}}$	sign $s_{\bar{\varphi}}$	bin	$\bar{A}_{\hat{T}}$	yie.	$m^2_{K\pi} - m^2_{K*} < 0$			$m^2_{K\pi} - m^2_{K*} > 0$		
					bin	$\bar{A}_{\hat{T}}$	yie.	bin	$\bar{A}_{\hat{T}}$	yie.
$- - +$	$-$	0	-13.2 ± 9.5	115	0	-21.9 ± 12.9	56	8	-8.0 ± 13.2	63
	$+$			151			88			74
$- - -$	$-$	1	3.2 ± 9.8	129	1	-1.6 ± 20.7	28	9	4.0 ± 11.2	99
	$+$			121			28			92
$- + +$	$-$	2	23.9 ± 10.0	149	2	18.9 ± 17.4	47	10	30.2 ± 12.2	105
	$+$			91			32			56
$- + -$	$-$	3	3.2 ± 7.8	204	3	5.0 ± 13.7	67	11	0.2 ± 9.4	136
	$+$			191			61			136
$+ - +$	$-$	4	24.3 ± 9.0	184	4	26.1 ± 16.3	57	12	22.7 ± 10.7	129
	$+$			112			33			81
$+ - -$	$-$	5	14.9 ± 8.6	186	5	21.9 ± 22.3	29	13	14.2 ± 8.8	177
	$+$			138			19			133
$+ + +$	$-$	6	-4.9 ± 8.6	154	6	-15.3 ± 11.4	78	14	6.4 ± 13.2	55
	$+$			170			106			48
$+ + -$	$-$	7	6.8 ± 6.6	294	7	2.8 ± 8.4	175	15	10.2 ± 9.5	147
	$+$			257			165			119

Table: The same as TABLE 2 but for $\overline{B^0} \to p\bar{p}K^-\pi^+$.

Accessible angular correlations based on the data in LHCb's paper

$j_a \backslash j_b$	0	1	2
0	$\Psi_0^{00} = 1$ trivial	$\Psi_0^{01} c_{\theta_b}$	$\Psi_0^{02} = \frac{1}{2}(c_{\theta_b}^2 - 1)$ ×
1	$\Psi_0^{10} = c_{\theta_a}$	$\Psi_0^{11} = c_{\theta_a} c_{\theta_b}$ $\Psi_1^{11} = s_{\theta_a} s_{\theta_b} c_{\varphi}$ $\Phi_1^{11} = s_{\theta_a} s_{\theta_b} s_{\varphi}$	$\Psi_0^{12} = \frac{1}{2} c_{\theta_a}(3c_{\theta_b}^2 - 1)$ × $\Psi_1^{12} = s_{\theta_a} s_{\theta_b} c_{\theta_b} c_{\varphi}$ $\Phi_1^{12} = s_{\theta_a} s_{\theta_b} c_{\theta_b} s_{\varphi}$
2	$\Psi_0^{20} = \frac{1}{2}(3c_{\theta_a}^2 - 1)$ ×	$\Psi_0^{21} = \frac{1}{2}(3c_{\theta_a}^2 - 1)c_{\theta_b}$ × $\Psi_1^{21} = s_{\theta_a} c_{\theta_a} s_{\theta_b} c_{\varphi}$ $\Phi_1^{21} = s_{\theta_a} c_{\theta_a} s_{\theta_b} s_{\varphi}$	$\Psi_0^{22} = \frac{1}{4}(3c_{\theta_a}^2 - 1)(3c_{\theta_b}^2 - 1)$ × $\Psi_1^{22} = s_{\theta_a} c_{\theta_a} s_{\theta_b} c_{\theta_b} c_{\varphi}$ $\Phi_1^{22} = s_{\theta_a} c_{\theta_a} s_{\theta_b} c_{\theta_b} s_{\varphi}$ $\Psi_2^{22} = \frac{3}{8} s_{\theta_a}^2 s_{\theta_b}^2 c_{2\varphi}$ × $\Phi_2^{22} = \frac{3}{8} s_{\theta_a}^2 s_{\theta_b}^2 s_{2\varphi}$

Accessible angular correlations based on the data in LHCb's paper

j_a \ j_b	0	1	2
0		$\Psi_0^{01} c_{\theta_b}$	
1	$\Psi_0^{10} = c_{\theta_a}$	$\Psi_0^{11} = c_{\theta_a} c_{\theta_b}$ $\Psi_1^{11} = s_{\theta_a} s_{\theta_b} c_\varphi$ $\Phi_1^{11} = s_{\theta_a} s_{\theta_b} s_\varphi$	$\Psi_1^{12} = s_{\theta_a} s_{\theta_b} c_{\theta_b} c_\varphi$ $\Phi_1^{12} = s_{\theta_a} s_{\theta_b} c_{\theta_b} s_\varphi$
2		$\Psi_1^{21} = s_{\theta_a} c_{\theta_a} s_{\theta_b} c_\varphi$ $\Phi_1^{21} = s_{\theta_a} c_{\theta_a} s_{\theta_b} s_\varphi$	$\Psi_1^{22} = s_{\theta_a} c_{\theta_a} s_{\theta_b} c_{\theta_b} c_\varphi$ $\Phi_1^{22} = s_{\theta_a} c_{\theta_a} s_{\theta_b} c_{\theta_b} s_\varphi$ $\Phi_2^{22} = \frac{3}{8} s_{\theta_a}^2 s_{\theta_b}^2 s_{2\varphi}$

$\mathcal{Y}_\sigma^{j_a j_b}$	Ψ_0^{00}	Ψ_0^{01}	Ψ_0^{10}	Ψ_0^{11}	Ψ_1^{11}	Φ_1^{11}		stat. err.	sys. err.
$A_{CP}^{\mathcal{Y}_\sigma^{j_a j_b}}$	5.8	8.5	-5.6	-2.8	2.5	-4.0		2.07	0.21
$\tilde{A}_{CP}^{\mathcal{Y}_\sigma^{j_a j_b}}$	/	**10.7**	/	**10.0**	-0.0	-0.5		2.05	0.21
$\mathcal{Y}_\sigma^{j_a j_b}$	Ψ_1^{12}	Φ_1^{12}	Ψ_1^{21}	Φ_1^{21}	Ψ_1^{22}	Φ_1^{22}	Φ_2^{22}	stat. err.	sys. err.
$A_{CP}^{\mathcal{Y}_\sigma^{j_a j_b}}$	**9.2**	-0.8	-1.7	-5.6	0.4	-2.0	-3.4	2.07	0.21
$\tilde{A}_{CP}^{\mathcal{Y}_\sigma^{j_a j_b}}$	/	/	-4.3	-2.4	/	/	/	2.05	0.21

Table: Decay angular correlation CPAs in unit of % calculated with the event yields extracted from the data of LHCb.

$$A_{CP}^{\Psi_0^{00}} \equiv \frac{1}{N+\overline{N}} \Big[(+115+151+129+121+149+91+204+191 +184+112+186+138+154+170+294+257)_{B^0} -(\cdots)_{\overline{B^0}}\Big] = 5.8 \pm 2.1.$$

$$A_{CP}^{\Psi_1^{12}} \equiv \frac{1}{N+\overline{N}} \Big[(-115+151+129-121+149-91-204+191 +184-112-186+138-154+170+294-257)_{B^0} -(\cdots)_{\overline{B^0}}\Big] = 9.2 \pm 2.1.$$

j_a \ j_b	0	1	2
0	$\Psi_0^{00} = 1$ trivial	$\boldsymbol{\Psi_0^{01} = c_{\theta_b}}$	$\Psi_0^{02} = \frac{1}{2}(c_{\theta_b}^2 - 1) \times$
1	$\Psi_0^{10} = c_{\theta_a}$	$\boldsymbol{\Psi_0^{11} = c_{\theta_a} c_{\theta_b}}$ $\Psi_1^{11} = s_{\theta_a} s_{\theta_b} c_\varphi$ $\Phi_1^{11} = s_{\theta_a} s_{\theta_b} s_\varphi$	$\Psi_0^{12} = \frac{1}{2} c_{\theta_a}(3c_{\theta_b}^2 - 1) \times$ $\Psi_1^{12} = s_{\theta_a} s_{\theta_b} c_{\theta_b} c_\varphi$ $\Phi_1^{12} = s_{\theta_a} s_{\theta_b} c_{\theta_b} s_\varphi$
2	$\Psi_0^{20} = \frac{1}{2}(3c_{\theta_a}^2 - 1) \times$	$\Psi_0^{21} = \frac{1}{2}(3c_{\theta_a}^2 - 1) c_{\theta_b} \times$ $\Psi_1^{21} = s_{\theta_a} c_{\theta_a} s_{\theta_b} c_\varphi$ $\Phi_1^{21} = s_{\theta_a} c_{\theta_a} s_{\theta_b} s_\varphi$	$\Psi_0^{22} = \frac{1}{4}(3c_{\theta_a}^2 - 1)(3c_{\theta_b}^2 - 1) \times$ $\Psi_1^{22} = s_{\theta_a} c_{\theta_a} s_{\theta_b} c_{\theta_b} c_\varphi$ $\Phi_1^{22} = s_{\theta_a} c_{\theta_a} s_{\theta_b} c_{\theta_b} s_\varphi$ $\Psi_2^{22} = \frac{3}{8} s_{\theta_a}^2 s_{\theta_b}^2 c_{2\varphi} \times$ $\Phi_2^{22} = \frac{3}{8} s_{\theta_a}^2 s_{\theta_b}^2 s_{2\varphi}$

interf. dynamics of the three large CPAs

- $\boldsymbol{\Psi_0^{01}}$: FB-CPA, interf. $K^*(892)$ and a scalar.
- $\boldsymbol{\Psi_0^{11}}$: two-fold FB-CPA, interf. $K^*(892)$ and a scalar, meanwhile, $0^\pm$ and $1^\mp$.
- Ψ_1^{12}: Left-Right Asymmetry CPA, interf. $0^\pm$ and $1^\mp$ in $p\bar{p}$ side

Why LHCb missed CPA in this baryon-production process

- obvious: TPA-CPAs are not large enough
- extracting CPAs in each of the small bins suffers from low statistics issue
- different kind of angular distributions are correlated in different ways, a simple summing up of the events in different bins will simply missing most of the angular correlations.

Why Full angular-correlation analysis of CPV is a powerful tool

- Full angular analysis, large CPAs may hide in angular-correlation other than TPAs
- collecting all bins for each observables, overcome low statistic issue
- The data of the bins are combined in non-trivial ways, overcome the cancellation problems.

methods \ features	statistical significance	inferring dynamics	model-independent	efficiency
regional CPA in Dalitz	×	×	✓	✓
amplitude analysis	✓	✓	×	×
energy test	✓	×	✓	×
full angular-correlation	✓	✓	✓	✓

4 summary and outlook

summary and outlook

- extremely strong evidence of CPV in $B^0 \to p\bar{p}K^+\pi^-$, CPA$\sim 10\%$
- Full analysis of angular-correlated CPA is a powerful tool,
- opportunities for CPV investigation in charmed sectors and more;
- challenges on theo. side: 1) Pres. Calc. 2)aim at right observables

features / methods	statistical significance	inferring dynamics	model-independent	efficiency
regional CPA in Dalitz	×	×	✓	✓
amplitude analysis	✓	✓	×	×
energy test	✓	×	✓	×
full angular-correlation	✓	✓	✓	✓

Thank you for your attentions!